

# An ice core derived 1013-year catchment scale annual rainfall reconstruction in subtropical eastern Australia

Carly R. Tozer<sup>1,2</sup>, Tessa R. Vance<sup>1</sup>, Jason L. Roberts<sup>3,1</sup>, Anthony S. Kiem<sup>2</sup>, Mark A. J. Curran<sup>3,1</sup>, Andrew D. Moy<sup>3,1</sup>

[1]{Antarctic Climate & Ecosystems Cooperative Research Centre, University of Tasmania, Hobart, Tasmania 7001, Australia}

[2]{Centre for Water, Climate and Land Use, University of Newcastle, Callaghan, NSW 2308, Australia}

[3]{Australian Antarctic Division, Kingston, Tasmania 7050, Australia}

Correspondence to: C. R. Tozer ([carly.tozer@utas.edu.au](mailto:carly.tozer@utas.edu.au))

## Abstract

Paleoclimate research indicates that the Australian instrumental climate record (~100 years) does not cover the full range of hydroclimatic variability that is possible. To better understand the implications of this on catchment-scale water resources management, a 1013-year (1000-2012 CE) annual rainfall reconstruction was produced for the Williams River catchment in coastal eastern Australia. No high resolution paleoclimate proxies are located in the region and so a teleconnection between summer sea salt deposition recorded in ice cores from East Antarctica and rainfall variability in eastern Australia was exploited to reconstruct the catchment-scale rainfall record. The reconstruction shows that significantly longer and more frequent wet and dry periods were experienced in the preinstrumental compared to the instrumental period. This suggests that existing drought and flood risk assessments underestimate the true risks due to the reliance on data and statistics obtained from only the instrumental record. This raises questions about the robustness of existing water security and flood protection measures and has serious implications for water resources management, infrastructure design, and catchment planning. The method used in this proof of concept study is transferable and enables similar insights into the true risk of flood/drought to be gained for other paleoclimate proxy poor regions for which suitable remote teleconnected proxies exist. This will lead to improved understanding and ability to deal with the impacts of multidecadal to centennial hydroclimatic variability.

# 1   **1   Introduction**

2   Water and catchment management systems (e.g. drought and flood mitigation strategies) and  
3   water resources infrastructure have traditionally been designed based on the trends, patterns  
4   and statistics revealed in relatively short instrumental climate records (i.e. for Australia usually  
5   less than 100 years of data recorded post-1900) (Verdon-Kidd and Kiem, 2010; Ho et al., 2014;  
6   Cosgrove and Loucks, 2015; Razavi et al., 2015). This is a concern as Australian paleoclimate  
7   research suggests that instrumental climate records are not representative of the true range of  
8   hydroclimatic variability possible (Verdon-Kidd and Kiem, 2010; Gallant and Gergis, 2011;  
9   Kiem and Verdon-Kidd, 2011; Ho et al., 2014; Ho et al., 2015a, b; Razavi et al., 2015; Vance  
10   et al., 2015). For example, paleoclimate archives show evidence of droughts of longer duration  
11   than the three major droughts that have affected eastern Australia over the instrumental period  
12   – the Federation drought (~1895-1902), World War II drought (~1937-1945) and Millennium  
13   or “Big Dry” drought (~1997 to 2009) (Gergis et al., 2012; Vance et al., 2013; Allen et al.,  
14   2015; Vance et al., 2015).

15   Sources for paleoclimate proxy data include tree rings, coral skeletons, ice cores, speleothems  
16   (cave deposits), sediments and documentary evidence (Ho et al., 2014). Ideally, the climate  
17   proxy archives are located in the region of interest but in areas where proxy records are sparse  
18   or of low resolution, remote proxies are a viable alternative (Ho et al., 2014). Remote proxies  
19   exploit circulation teleconnections that link one region to another and are calibrated over the  
20   instrumental period, to develop paleoclimate reconstructions (e.g. rainfall, streamflow) for the  
21   target region (e.g. Verdon and Franks, 2007; McGowan et al., 2009; van Ommen and Morgan,  
22   2010; Vance et al., 2013; Vance et al., 2015). When using remote proxies the assumption is  
23   that large-scale climate processes driving climate variability at the location of the paleoclimate  
24   proxy also drive a high proportion of climate variability at the region of interest (Gallant and  
25   Gergis, 2011). For example, van Ommen and Morgan (2010) identified a relationship between  
26   precipitation (snowfall) recorded in ice cores from coastal Antarctica and rainfall in southwest  
27   Western Australia over the instrumental period, inferring rainfall variability in the region for  
28   the past 750 years. Similarly, Lough (2011) found significant correlations between coral  
29   luminescence intensity recorded in coral cores from the Great Barrier Reef and summer rainfall  
30   variability in northeast Queensland which enabled the multi-century coral record to be used to  
31   reconstruct Queensland summer rainfall back to the 18<sup>th</sup> century.

32   Another option is to use the link between large-scale ocean-atmospheric climate processes and  
33   climate variability in the region of interest to develop a paleoclimate reconstruction based on a

1 paleoclimate proxy of the climate process. For example, McGowan et al. (2009) reconstructed  
2 annual inflows in the Murray River back to 1474 CE from a reconstruction of the Pacific  
3 Decadal Oscillation (PDO) based on the previously identified relationship between the PDO  
4 and streamflow in southeast Australia (e.g. Power et al., 1999a; Power et al., 1999b; Kiem et  
5 al., 2003; Kiem and Franks, 2004; Verdon et al., 2004). A similar approach was also followed  
6 by Verdon and Franks (2006, 2007) and Henley et al. (2011).

7 Vance et al. (2013) and Vance et al. (2015) used a hybrid of the approaches discussed above.  
8 Vance et al. (2013) developed a millennial length rainfall reconstruction for subtropical eastern  
9 Australia by exploiting a relationship between the region's annual rainfall and the summer sea  
10 salt record (see Sect. 3) from the Law Dome ice core, East Antarctica (Fig. 1). Of key  
11 importance is that the strength of the relationship during the instrumental period (in this case  
12 1889-2009) varies synchronously with the Interdecadal Pacific Oscillation (IPO) (Power et al.,  
13 1999a; Power et al., 1999b), the basin-wide expression of the PDO, with increased correlations  
14 found during IPO positive phases (Vance et al., 2013; Vance et al., 2015). The IPO represents  
15 decadal sea surface temperature (SST) variability across the Pacific Ocean whereby a positive  
16 IPO phase is associated with warming across the tropical Pacific and cooling of the north and  
17 south Pacific; the opposite occurs during the negative phase (Power et al., 1999a). The most  
18 recent defined complete IPO phases are two positive phases (~1924-1941, ~1979-1997) and  
19 one negative phase (~1947-1975) (Power et al., 1999a; Kiem et al., 2003; Kiem and Franks,  
20 2004; Verdon et al., 2004).

21 Vance et al. (2015) demonstrated that during the IPO negative phase there is a predominantly  
22 zonal pressure pattern across the high- to mid-latitudes which switches to a more meridional  
23 pattern in IPO positive. Folland et al. (2002) also found that during the IPO positive phase, the  
24 mean position of the South Pacific Convergence Zone (SPCZ) (usually bounded by Samoa and  
25 Fiji) is displaced northeast. This northeast displacement is associated with a more meridional  
26 circulation pattern and enhances the link between eastern Australia and mid- to high-latitude  
27 climate variability and hence explains the stronger relationship between sea salt recorded at  
28 Law Dome and rainfall in eastern Australia during the IPO positive phase. Based on their  
29 reconstruction of the IPO, Vance et al. (2015) could therefore identify periods in time (i.e.  
30 positive IPO phases) where they had greater confidence in the rainfall reconstruction. A key  
31 finding from Vance et al. (2015) was the identification of a century of IPO positive aridity  
32 (1102-1212 CE), including evidence of a 39 year drought in southeast Queensland, which is  
33 well outside the bounds of instrumental drought duration. This illustrates the importance of

1 investigating climate variability over millennial time-scales, particularly in the Southern  
2 Hemisphere where many paleoclimate records only span the last two hundred to five hundred  
3 years (Neukom and Gergis, 2012). Indeed, it is evident that: (a) instrumental data are not long  
4 enough to allow for meaningful planning for climate variability; (b) paleodata, particularly at  
5 the millennial time-scale, offers an important insight into the climate beyond the instrumental  
6 period; and (c) there is a need to incorporate insights from paleodata into water resources  
7 planning and management.

8 Further work is also required to assess the robustness of the relationship between climate  
9 variability in East Antarctica, large-scale climate processes and eastern Australia, a region with  
10 limited local paleoclimate proxy data (Vance et al., 2013; Ho et al., 2014). Practical usefulness  
11 of the insights provided by the paleoclimate reconstructions for water resources management  
12 at the catchment scale also requires investigation. Therefore, the links between the Law Dome  
13 sea salt record, eastern Australian rainfall and the IPO are further explored in this paper through  
14 the development of a millennial length, annual resolution, catchment-scale rainfall  
15 reconstruction for the Williams River (WR) catchment (Fig. 1). The WR catchment is located  
16 on the eastern seaboard of New South Wales, east of the Great Dividing Range (Fig. 1). The  
17 eastern seaboard contains about half of Australia's population, and a proportionate amount of  
18 economic infrastructure and activity. The region has hydroclimate features that are distinct  
19 from the rest of Australia (e.g. Verdon and Franks, 2005; Timbal, 2010) and lacks high  
20 resolution paleoclimate proxies (Ho et al., 2014). This means there is significant vulnerability,  
21 uncertainty and knowledge gaps relating to flood and drought risk in eastern Australia. This  
22 recognition has recently motivated the development of the Eastern Seaboard Climate Change  
23 Initiative (ESCCI), to better understand the causes and impacts of current and future climate  
24 related risk in the region ([http://www.climatechange.environment.nsw.gov.au/About-climate-  
25 change-in-NSW/Evidence-of-climate-change/Eastern-seaboard-climate-change-initiative](http://www.climatechange.environment.nsw.gov.au/About-climate-change-in-NSW/Evidence-of-climate-change/Eastern-seaboard-climate-change-initiative)).

26 The WR catchment is of particular regional importance because it forms part of the  
27 conjunctive-use headworks scheme for potable water supply to ~600,000 people in Newcastle,  
28 the sixth largest residential region in Australia (Kiem and Franks, 2004; Mortazavi-Naeini et  
29 al., 2015).

30 In the following sections we present a description of the WR catchment location and relevant  
31 climate data, including a discussion of the link between Law Dome, East Antarctica and eastern  
32 Australia. We proceed with an investigation into the relationship between summer sea salts  
33 from Law Dome and rainfall in the WR catchment and follow with the development of a 1013-

1 year catchment-scale rainfall reconstruction (based on the Law Dome sea salt record) and  
2 discussion of the insights and implications emerging from this reconstruction.

3

## 4 **2 Rainfall variability in the Williams River catchment**

5 For the calibration data in this study we used daily 5 x 5 km gridded rainfall data obtained from  
6 the Australian Water Availability Project (AWAP) (Jones et al., 2009) for the period 1900-  
7 2010. The AWAP grid-cells overlapping the WR catchment were extracted and used to  
8 calculate catchment average monthly rainfall totals for the WR catchment. Due to known biases  
9 and uncertainty associated with gridded climate data (e.g. Tozer et al., 2012), the AWAP-based  
10 information was ground-truthed with data from a high quality (Lavery et al., 1997) rainfall  
11 gauge (61010) located within the WR catchment. The highest and most variable rainfall in the  
12 WR catchment is received from December to May (summer and autumn) (Figure 2) and the  
13 hydrological water year for the WR catchment is therefore defined as October to September in  
14 order to encompass this high rainfall period (pers. comm., Brendan Berghout, Senior Water  
15 Resources Engineer, Hunter Water Commission).

16 Rainfall variability in the WR catchment is influenced by the Great Dividing Range to the west  
17 (Figure 1) which provides orographic enhancement and the Tasman Sea to the east which  
18 brings moisture to the region (Pepler et al., 2014). Synoptic scale influences known as East  
19 Coast Lows (ECLs), marine or continental low pressure systems which tend to develop in the  
20 Tasman Sea, are responsible for much of the extreme weather (e.g. heavy rainfall, high winds)  
21 recorded in eastern New South Wales (Speer et al., 2009; Browning and Goodwin, 2013; Pepler  
22 et al., 2014b; Ji et al., 2015; Kiem et al., 2015; Twomey and Kiem, 2015b, a). Indeed, ECLs  
23 have been found to contribute 20-30% of annual rainfall in the WR region (Pepler et al., 2014a).  
24 In addition to these local influences several large-scale ocean-atmospheric processes influence  
25 rainfall in the WR catchment (e.g. Kiem and Franks, 2001, 2004; Risbey et al., 2009). The El  
26 Niño Southern Oscillation (ENSO) and IPO have been related to interannual to multidecadal  
27 variability in both WR rainfall and runoff (Kiem and Franks, 2001, 2004). Drier (wetter)  
28 catchment conditions typically occur during El Niño (La Niña) events and the IPO modulates  
29 both the frequency and magnitude of ENSO impacts such that drought risk is increased during  
30 IPO positive phases and flood risk is increased during IPO negative phases (Kiem and Franks,  
31 2001; Kiem et al., 2003; Kiem and Franks, 2004; Kiem and Verdon-Kidd, 2013). Indian Ocean

1 SSTs are also known to influence eastern Australian rainfall during winter and spring (Verdon  
2 and Franks, 2005; Risbey et al., 2009).

3 In addition, the Subtropical Ridge (STR) and Southern Annular Mode (SAM) impact rainfall  
4 variability in the eastern seaboard (e.g. Risbey et al., 2009; Ho et al., 2012; Whan et al., 2013).  
5 A positive SAM phase has been related to increased daily rainfall in summer and spring  
6 (Hendon et al., 2007; Risbey et al., 2009) while variability in the position of the STR is  
7 significantly correlated with rainfall in the eastern seaboard. That is, a shift south of the STR  
8 is associated with increased rainfall in the region (Timbal, 2010; Whan et al., 2013). Variability  
9 in the intensity of the STR is also related to rainfall variability in the eastern seaboard though  
10 to a lesser extent than variability in the STR position (Timbal, 2010).

11

### 12 **3 The Law Dome-eastern Australia rainfall proxy**

#### 13 **3.1 Law Dome ice core site details**

14 Law Dome is a small, coastal icecap located in Wilkes Land, East Antarctica (Figure 1) and  
15 the site of the Dome Summit South (DSS) ice core which spans around 90,000 years (Roberts  
16 et al., 2015). DSS has high annual snowfall of around 0.63 m (water equivalent) which allows  
17 for a monthly resolution record in the upper portion of the core and highly accurate dating (van  
18 Ommen and Morgan, 1997; Vance et al., 2013; Roberts et al., 2015). The ice core was dated  
19 by counting annual layers with known volcanic horizons used to establish dating accuracy  
20 (Plummer et al., 2012). As a result, the Law Dome record was dated with absolute accuracy  
21 from 1807-2009 Common Era (CE) and with  $\pm 1$  year error from 894-1807 CE. The sea salt  
22 record used here was produced using trace ion chromatography from 2.5-5 cm sub-samples of  
23 the ice cores (Curran et al., 1998; Palmer et al., 2001). The Law Dome summer (December-  
24 March) sea salts ( $LD_{SSS}$ ) were extracted from the full record and used by Vance et al. (2013)  
25 and Vance et al. (2015) as a rainfall proxy for eastern Australia. Here we use a slightly extended  
26  $LD_{SSS}$  record to cover the epoch 1000-2012 CE using the improved composite record of  
27 Roberts et al. (2015).

### 3.2 The link between sea salt deposition at Law Dome and large-scale ocean-atmospheric processes

The climate signals recorded in the Law Dome ice core are driven by large-scale ocean-atmospheric processes rather than local factors (Bromwich, 1988; Delmotte et al., 2000; Masson-Delmotte et al., 2003; Vance et al., 2013). The southern Indian Ocean is the main source of moisture delivered to Law Dome (Delmotte et al., 2000; Masson-Delmotte et al., 2003) and sea salt deposition is related to the mid-latitude westerly winds (associated with the SAM) in the Indian and Pacific sectors of the Southern Ocean (Goodwin et al., 2004; Vance et al., 2015). Seasonal to annual scale SST anomalies in the equatorial Pacific are known to propagate to high southern latitudes (Károly, 1989; Mo and Higgins, 1998; Ding et al., 2012). The resulting circumpolar geopotential height and zonal wind anomalies influence the SAM (L'Heureux and Thompson, 2006), and ultimately deliver sea salt aerosols to coastal Antarctica (Vance et al., 2013). Indeed, Vance et al. (2013) found a significant correlation between ENSO-related SST variability in the central-western equatorial Pacific and LD<sub>SSS</sub>, with low summer sea salt years associated with El Niño events over the period 1889-2009. Furthermore, spectral analysis of the 1010-year LD<sub>SSS</sub> record found significant ( $p < 0.01$ ) spectral features in the 2-7 year ENSO band. Similar to the LD<sub>SSS</sub> rainfall proxy discussed previously, the LD<sub>SSS</sub> ENSO proxy varies decadal, coherent with the IPO, with a stronger relationship during IPO positive phases (Vance et al., 2013; Vance et al., 2015).

It is thus clear that the ocean-atmospheric processes associated with sea salt deposition at Law Dome (e.g. IPO, ENSO, SAM and variability in the Indian Ocean) are the same as those that influence rainfall variability in the WR catchment (discussed in Sect. 2). We can therefore expect LD<sub>SSS</sub> to explain some variability in the rainfall in the WR catchment.

### 4 Investigating the relationship between LD<sub>SSS</sub> and rainfall in the Williams River catchment

Vance et al. (2013) found a relationship between LD<sub>SSS</sub> and the prior January-December rainfall west of the Great Dividing Range. The region of interest in this study is further south and east of the Great Dividing Range so we needed to re-evaluate if this temporal offset was appropriate. This re-evaluation was via a damped least-squares regression between AWAP grid-cell data and the LD<sub>SSS</sub> record using the Marquardt-Levenberg method, a method capable of multi-variate and non-linear regression. Although it was only used for uni-variate linear

1 regression here, the method was selected for compatibility with planned future work. For every  
2 AWAP grid-cell in New South Wales we performed linear least squares regression between  
3 the LD<sub>SSS</sub> record and 12 month averaged rainfall over a 24 month lead/lag range centred about  
4 the summer sea salt period (December-March). The regression coefficients for each lead/lag  
5 were used to generate an estimated spatial rainfall time-series. The Pearson correlation  
6 coefficient between the estimated rainfall and AWAP rainfall for each grid-cell was then assessed  
7 for each lead/lag. This process allowed us to determine the seasonal window for rainfall that  
8 optimised the WR rainfall-LD<sub>SSS</sub> relationship in order to optimise the utility of the LD<sub>SSS</sub>  
9 record.

10 From the lead/lag analysis, October-September and November-October annual rainfall in the  
11 region encompassing the WR catchment was found to have the highest and most spatially  
12 coherent relationship with LD<sub>SSS</sub>. We present the October-September rainfall/LD<sub>SSS</sub>  
13 correlations (Figure 3) as this period also corresponds to the water year in the Newcastle region  
14 (discussed in Sect. 2) and hence all further analysis is based on the 12 month rainfall totals  
15 calculated from October-September.

16 Figure 3 shows spatial maps of the magnitude of the correlations between October-September  
17 WR rainfall and LD<sub>SSS</sub> for the 1900-2010 (i.e. October 1900-September 2010) period as well  
18 as subsets for the different IPO phases. For comparison Figure 3a-e are inset with maps for the  
19 January-December rainfall/LD<sub>SSS</sub> correlations, the analysis period used in Vance et al. (2013)  
20 and Vance et al. (2015). Figure 3f indicates the 13 year moving window correlations between  
21 LD<sub>SSS</sub> and October-September for rainfall recorded at gauge 61010 and the AWAP WR  
22 catchment average in order to identify low frequency variability associated with the IPO. The  
23 Pearson correlation coefficients between LD<sub>SSS</sub> and October-September annual rainfall  
24 recorded at gauge 61010 and the AWAP WR catchment average for the full record and IPO  
25 phases are presented in Table 1. The significance of the relationships are confirmed using  
26 bootstrap confidence intervals based on the method of Mudelsee (2003).

27 The insets of Figures 3a-e reveal low correlations in the WR catchment region. The highest  
28 correlations occur in inland New South Wales and into southeast Queensland, the focus region  
29 of Vance et al. (2013) and Vance et al. (2015). However, when the correlation is aligned with  
30 the WR catchment water year (October-September) we see a shift in the region of significant  
31 correlation (Figure 3a) to coastal New South Wales and in particular, large parts of the eastern  
32 seaboard. Importantly, correlations significant at the 99% level are seen over the WR catchment  
33 region. Rainfall at gauge 61010 and AWAP catchment average show significant correlations



1 with LD<sub>SSS</sub> (Pearson correlation coefficients of 0.29 and 0.28 respectively) over the 1900-2010  
2 period (Table 1).

3 As expected, based on the results of Vance et al. (2013) and Vance et al. (2015) (discussed in  
4 Sect. 3), the strength of the correlation between October-September rainfall and LD<sub>SSS</sub> varies  
5 decadal. Figure 3b-c indicate that the relationship between the variables is stronger during  
6 the IPO positive phases relative to the negative phase. Figure 3d-e and the results in Table 1,  
7 however, suggest that although the relationship between October-September rainfall and LD<sub>SSS</sub>  
8 is stronger in IPO positive phase, this increase in strength relative to IPO negative and the full  
9 record (1900-2010) is primarily due to the very high correlation in the second IPO positive  
10 phase (1979-1997). In fact, the correlation between rainfall recorded at gauge 61010 and LD<sub>SSS</sub>  
11 during the IPO negative phase is greater than the correlation in the first IPO positive phase  
12 (Table 1). Figure 3f further highlights that an increase (decrease) in the strength of the LD<sub>SSS</sub>-  
13 WR rainfall relationship is not always synchronous with IPO positive (negative) phases.

14 This result appears to be in contrast to Vance et al. (2013) and Vance et al. (2015) who found  
15 a clear link between IPO phase and LD<sub>SSS</sub>-January-December rainfall in southeast Queensland  
16 and northeast New South Wales (west of the Great Dividing Range). That is, the correlation  
17 between these variables was poor during the IPO negative phase, yet was significant for both  
18 positive phases. Vance et al. (2013) and Vance et al. (2015) used calendar year rainfall as  
19 opposed to a more catchment specific analysis period used in this study. Another key difference  
20 is that the focus region here is further south, on the coast and under the orographic influence  
21 of the Great Dividing Range. Furthermore, although interdecadal and interannual tropical  
22 Pacific Ocean variability (e.g. ENSO and IPO) has been found to impact the whole of Australia  
23 at various times of the year (e.g. Power et al., 1999a; Risbey et al., 2009), the amount of rainfall  
24 variability explained by these processes reduces to the south while climate mechanisms  
25 stemming from the mid- to high-latitudes (e.g. SAM and the STR, discussed in Sect. 2) increase  
26 their influence on rainfall variability (Risbey et al., 2009).

27 In addition, as mentioned previously, around one quarter of annual rainfall received in the WR  
28 catchment results from ECLs (Pepler et al., 2014a). In 1950 and 1955 the Newcastle region  
29 experienced heavy rainfall and floods as a result of severe ECLs (Callaghan and Helman, 2008;  
30 Callaghan and Power, 2014) and indeed eastern Australia in general was subject to an increase  
31 in intense storm activity between the 1940s and 1970s (Callaghan and Power, 2011; Browning  
32 and Goodwin, 2015). The relationship between LD<sub>SSS</sub> and rainfall in the WR catchment could  
33 not be expected to hold during these short duration but intense local-scale weather events and

1 remote proxy records in general are usually incapable of resolving events like these. As such,  
2 this period of elevated intense storm activity may explain the marked reduction (and change of  
3 sign) in the correlation between LD<sub>SSS</sub> and rainfall in the WR catchment in the early 1950s  
4 (Figure 3f). ECL variability has been related to the IPO, with Speer (2008) finding that during  
5 the second IPO positive phase (i.e. 1979-1997) there was a decrease in ECLs relative to IPO  
6 negative. This would correspond to a reduction in ECL-related rainfall over New South Wales  
7 in the most recent IPO positive phase and is further evidence that these short duration, chaotic  
8 events affect the relationship between LD<sub>SSS</sub> and rainfall in the WR catchment.

9 Indeed, a better understanding of the role of ECLs and also the relative influence of ENSO,  
10 IOD, SAM, STR and other large-scale processes on rainfall in the WR catchment (as is  
11 currently being investigated as part of the ESCCI project) will undoubtedly improve our  
12 understanding of the variability in the strength of the LD<sub>SSS</sub>-WR rainfall teleconnection. It  
13 should also be noted that one of the key difficulties in understanding the non-stationarity in the  
14 climate of the Southern Hemisphere is the lack of quality atmospheric/oceanic data in the  
15 Southern Ocean in the pre-1979 satellite era, particularly in the Indian/West Pacific sector. It  
16 is likely that more high resolution ice core records from the Indian Ocean sector of East  
17 Antarctica will assist in filling this data gap (Vance et al., 2016). Underpinning the above issue  
18 is that variability in the Australian climate record can be up to centennial scale which cannot  
19 be resolved using relatively short instrumental datasets (Gallant et al., 2013). Ultimately, for  
20 the purposes of this initial reconstruction, we have assumed stationarity in the LD<sub>SSS</sub>-Williams  
21 River rainfall relationship.

22

## 23 **5 Reconstructing rainfall in the Williams River catchment**

### 24 **5.1 Development of the Williams River rainfall reconstruction**

25 The linear regression coefficients determined for the full 1900-2010 instrumental calibration  
26 period (Sect. 4) were applied to the 1000-2012 CE LD<sub>SSS</sub> data to produce 1013 years of rainfall  
27 data for each AWAP grid-cell in the WR catchment. This grid-cell data was then spatially  
28 averaged to produce a WR catchment average rainfall reconstruction time-series.

## 5.2 Comparing the catchment average rainfall reconstruction with instrumental (AWAP) data

A comparison between the AWAP catchment average and reconstructed WR catchment rainfall over the instrumental period (1900-2010) is presented in Figure 4. The instrumental mean and pattern of peaks and troughs in the recorded rainfall is well represented in the reconstruction but the range of variability is underestimated. While the magnitude of the extremes is important, the key focus is that the reconstruction captures the duration and timing of wet and dry periods. The thinking behind this is that a short, but extreme (in terms of rainfall deficit) drought, for example, will have less severe implications on water security in a catchment than a drought of long duration with consistently below average (but not necessarily extremely below average) rainfall. Encouragingly, periods post-1900 that are known to be associated with droughts and flooding in the WR catchment are identified in the reconstruction e.g. the World War II drought in the late 1930s, the Millennium drought in the 1990s to 2000s, and the flood dominated 1950s and 1960s (e.g. Verdon-Kidd and Kiem, 2009; Gallant et al., 2012; Callaghan and Power, 2014).

The rainfall reconstruction captures around 10% of the rainfall variability in the WR catchment for the full 1900-2010 instrumental period (Table 1). In terms of IPO phases, it is clear that the reconstruction is in better agreement with the instrumental record for the most recent IPO positive phase (1979-1997) relative to the first IPO positive phase and the IPO negative phase. This is no surprise given the higher correlation between LD<sub>SSS</sub> and Williams River rainfall in the recent IPO positive period i.e. LD<sub>SSS</sub> variability captures around 40% of the Williams River rainfall variability (Table 1). Influences on the stationarity of the LD<sub>SSS</sub>-WR rainfall relationship were discussed in Sect. 4.

Table 2 presents the Root Mean Square Error (RMSE) and reduction in error (RE) between the rainfall reconstruction and 12 month average (October-September) rainfall recorded at gauge 61010 and the AWAP WR catchment average for the 1900-2010 period and IPO phases. An RE value greater than zero indicates that the reconstruction is skilful and has better predictive skill than climatology (Cook, 1992). While improved RMSE and RE statistics were recorded for the most recent IPO positive (1979-1997) relative to the first IPO positive and IPO negative phases, it is clear that the reconstruction has skill across the 1900-2010 instrumental period. For the full instrumental record, the reconstruction has an RMSE of around 25% of the annual instrumental rainfall with an RE value greater than zero.

### 5.3 A millennial rainfall reconstruction for the WR catchment

Figure 5 presents the 1013-year rainfall reconstruction produced for the WR catchment. From the 10-year smoothed record it is evident that there have been multi-year periods of either above or below average rainfall. A multi-century dry period is evident from around 1100-1250 CE while two similarly persistent wet periods are seen from around 1400-1600 CE and 1800-1900 CE.

As mentioned previously, few rainfall proxy records exist in eastern Australia. Those that do tend to be outside of the Eastern Seaboard region in climate regimes that have significant differences, cover different time periods or are at varying (lower) resolutions, which limits the ability to compare them to the reconstruction provided here. However, broad commonalities can be discussed. Heinrich et al. (2009) developed a 154-year rainfall reconstruction for Brisbane, located near the northern boundary of the eastern seaboard, from red cedar tree-ring analysis. Since the record commences in 1854, which is within the instrumental period for the Brisbane region (Heinrich et al., 2009), the utility of this record for comparison here is limited. Nevertheless, the authors found drier periods in the 1880s, 1900-1920, most of 1940s and 1990s and wetter periods in the 1860s, 1890s, 1930s and 1970s which fits with the results shown in Figure 5 if the reconstruction is compared with the instrumental mean as opposed to the full 1000-2012 mean. Although not a rainfall reconstruction, an aridity index of wet and dry periods is available based on speleothems from the Wombeyan Caves, located in the Sydney region (i.e. within the eastern seaboard) for the 749 BCE to 2001 CE period (McDonald, 2005; McDonald et al., 2009; McDonald et al., 2013). Dry epochs evident in the Wombeyan aridity index, for the period where it overlaps with the WR reconstruction, include late-1100s, around 1500, mid-1700s, and early-1900s which is consistent with the WR reconstruction illustrated in Figure 5. Similarly, the Wombeyan record indicates epochs that were “not dry” include the early-1400s, 1510-1600, early-1700s, and late-1800s, which is again consistent with the results presented in Figure 5 (McDonald, 2005; McDonald et al., 2009; McDonald et al., 2013; Ho et al., 2015a, b).

In addition, Gergis et al. (2012) produced a multi-proxy based annual rainfall reconstruction for a broad southeast portion of Australia for the 1783-1988 CE period, finding the 20<sup>th</sup> century to be drier during their ~200 year analysis period. Similarly, Figure 5 shows that the recent era (1900-present) is relatively dry in the post-1783 time period and also in the context of the last 1000 years, though it is not unprecedented. For the 1685-1981 CE period, Lough (2011) found drier and less variable summer rainfall in far northeast Queensland between 1760-1850 and a

1 tendency for a wetter climate from the mid-1850s to 1900 from their coral based rainfall proxy.  
2 Likewise, the reconstruction shown here tends to indicate a drier period post-1700, switching  
3 to a wetter regime from the late-1700s to the beginning of the 20<sup>th</sup> century.  
4 Ultimately we find good agreement with existing nearby rainfall reconstructions. This further  
5 validates the rainfall reconstruction presented here particularly in light of previously identified  
6 concerns with comparing it to other reconstructions in the eastern Australia region.

#### 7 **5.4 Implications for water resources management**

8 While Figure 5 gives insights into periods of above and below average rainfall, of particular  
9 interest for hydrological studies and water resources management is not just whether a year or  
10 sequence of years is above or below the long term average but whether a multiyear or  
11 multidecadal epoch is generally wet or dry even though some years within that epoch may be  
12 slightly below or above the long term average. For example, a year that is only 0.1 standard  
13 deviations above the average is unlikely to provide enough rainfall to break a drought or fill  
14 reservoirs. To account for this we define ‘wet’ and ‘dry’ years as (Eq. 1):

$$15 \text{ wet} = \text{years where rainfall} > \text{mean} - x \times \text{standard deviation} \quad (1)$$

$$16 \text{ dry} = \text{years where rainfall} < \text{mean} + x \times \text{standard deviation}$$

17 For example, for a standard deviation of 0.1 (and annual average of 1100 mm), the range is  
18 1092.6-1107.4 mm. That is, a wet year will be defined as any year with annual rainfall greater  
19 than 1092.6 mm and a dry year as any year with annual rainfall less than 1107.4 mm. Some  
20 years will be defined as both ‘wet’ and ‘dry’ but this methodology avoids a situation where a  
21 consistently wet (or dry) period is broken by a single year that is slightly below (or above) the  
22 mean.

23 Table 3 compares the persistence of the longest above and below average rainfall periods ( $x = 0$   
24 in Eq. 1), and ‘wet/dry’ periods ( $x = 0.1, 0.2, 0.3, 0.4, 0.5$  in Eq. 1) in the AWAP catchment  
25 average rainfall and the reconstruction. Note that the time periods identified in Table 3 should  
26 be considered in light of the  $\pm 1$  year dating uncertainty of the LD<sub>SSS</sub> record discussed in Sect.  
27 3.1. As shown in Table 3 (parts A and B) the reconstruction captures the dry periods, in terms  
28 of duration and timing, of the AWAP instrumental record well and also the duration of the  
29 longest wet periods. However, the timing of the wettest periods detected by the reconstruction  
30 is different to that seen in the AWAP record. As previously discussed this is likely due to the  
31 inability of the LD<sub>SSS</sub> reconstruction to characterise extreme local-scale synoptic activity in the

1 WR region (i.e. ECLs). Importantly, this also implies that the wettest epochs in the  
2 reconstruction may be an underestimation, as the reconstruction is least accurate during wet  
3 periods caused predominantly by local-scale influences (e.g. ECLs). In other words, wet  
4 periods associated with increased ECL activity (e.g. similar to the 1950s) are possible and the  
5 magnitude of rainfall associated with these events would be over and above the preinstrumental  
6 wet epochs suggested by the LD<sub>SSS</sub> reconstruction.

7 Figure 6 shows the duration of above and below average rainfall periods during each century  
8 since 1000 CE (and also for the whole 1013 year reconstruction period). To easily visualise the  
9 results, Figure 6 combines all durations > 15 years (information on all durations is included in  
10 Table S1 in the Supplementary Material). Figure 6 clearly shows that (a) some centuries are  
11 drier (more pink) than others (more blue) and (b) the most recent complete century (1900-  
12 1999), where the majority of our instrumental record comes from, is not representative of either  
13 the duration or frequency of periods of above or below average rainfall experienced pre-1900.

14 While the results in Figure 6 are important, of greater interest is the identification of the  
15 persistence of wet or dry periods even though some years within the otherwise dry (wet) regime  
16 were slightly wetter (drier) than average. Table 3 (part A and B) shows that using the threshold  
17 approach outlined in Eq. 1 does not noticeably change the duration of the longest wet or dry  
18 periods in the instrumental period. If dry and wet epochs, defined relative to the 1100.0 mm  
19 instrumental mean and using a standard deviation threshold of 0.3 (which is mid-range in the  
20 context of the 0.1-0.5 range of standard deviation thresholds assessed), are extracted from the  
21 preinstrumental reconstruction, a different story emerges (Table 3, part C). The results show  
22 that the longest dry epochs persist for up to 12 years instead of a maximum of 8 years post-  
23 1900 while wet epochs have lasted almost five times as long (maximum of 39 years  
24 preinstrumental compared to a maximum of 8 years in the instrumental period). A similar result  
25 is observed if the full reconstruction mean (1126.1 mm) is used to indicate wet or dry (Table  
26 3, part D), with both the dry and wet epochs persisting up to twice as long in the preinstrumental  
27 compared to the instrumental period. Figure 7 (and the associated Table S2 and Table S3 in the  
28 Supplementary Material) further illustrates this point (and the points made in relation to Figure  
29 6) by clearly showing that the proportion, frequency and duration of wet/dry epochs in the  
30 instrumental period (1900-1999) is not representative of either the overall situation throughout  
31 the last 1000 years or the situation in any century pre-1900. Also of interest is that some  
32 centuries tend to have short dry periods compared with long dry periods and vice-versa – e.g.  
33 the 15th and 16th century (Figure 7e and Figure 7f) compared to the 12th and 13th century

1 (Figure 7b and Figure 7c). The same can be said for wet periods. The variation in the  
2 distribution of dry/wet period duration between centuries further suggests that water resources  
3 management and planning based on the statistics of 100 years of data (or less) is problematic.

## 5 **6 Conclusions**

6 This study produced a 1013-year rainfall reconstruction for the WR catchment, a location  
7 without any local paleoclimate proxies. The strength of the relationship between  $LD_{SSS}$  and  
8 annual WR rainfall was found to vary decadal but, unlike Vance et al. (2013) and Vance et  
9 al. (2015), was not always coherent with the IPO. This is likely due to the different climate  
10 regime that the coastal WR catchment is subject to (e.g. likely more influence from mid-latitude  
11 processes) compared to the previous studies which were located further north and  
12 predominantly west of the Great Dividing Range. The WR catchment is also strongly  
13 influenced by local-scale coastal storms such as ECLs which may provide an explanation for  
14 the different relationship to the IPO, as well as the breakdown in the East Antarctic-WR  
15 teleconnection in periods associated with increased ECL activity (e.g. the 1950s).

16 Despite the acknowledged nonstationarity in the relationship (which is being further  
17 investigated in ongoing research) the relationship between  $LD_{SSS}$  and rainfall in the WR  
18 catchment is significant over the full 1900-2010 calibration period and indeed the  
19 reconstruction shows skill across this period. The reconstruction was found to agree well with  
20 identified dry/wet periods in other rainfall reconstructions in the eastern Australia region  
21 providing further validation. Ultimately, the  $LD_{SSS}$ -based reconstruction shows that the  
22 instrumental period (~1900-2010) is not representative of the proportion, frequency or duration  
23 of wet/dry epochs in any century in the preinstrumental era. This is consistent with recent  
24 independent studies focussed on Tasmania (Allen et al., 2015) and the Murray-Darling Basin  
25 (Ho et al., 2015a, b).

26 These findings provide compelling evidence that existing hydroclimatic risk assessment and  
27 associated water resources management, infrastructure design, and catchment planning in the  
28 WR catchment is flawed given the reliance on drought and flood statistics derived from post-  
29 1900 information. Figure 3 (and Fig. 4a in Vance et al. (2015)) suggest that the same is true for  
30 most of eastern Australia and indeed may also be the case for other regions in Australia that  
31 are identified as (or yet to be identified as) having similar teleconnections with East Antarctica  
32 e.g. southwest Western Australia (van Ommen and Morgan, 2010). Therefore, the robustness

1 of existing flood and drought risk quantification and management in eastern Australia is  
2 questionable and the insights from paleoclimate data need to be incorporated into catchment  
3 planning and management frameworks, especially given the multidecadal and centennial  
4 hydroclimatic variability demonstrated in this study

5

## 6 **Acknowledgements**

7 This work was supported by the Australian Government's Cooperative Research Centres  
8 Programme through the Antarctic Climate and Ecosystems Cooperative Research Centre (ACE  
9 CRC). The Australian Antarctic Division provided funding and logistical support for the DSS  
10 ice cores (AAS projects 4061 and 4062). The Centre for Water, Climate and Land Use at the  
11 University of Newcastle provided partial funding for Tozer's salary.

12

## 13 **References**

- 14 Allen, K. J., Nichols, S. C., Evans, R., Cook, E. R., Allie, S., Carson, G., Ling, F., and Baker,  
15 P. J.: Preliminary December–January inflow and streamflow reconstructions from tree rings  
16 for western Tasmania, southeastern Australia, *Water Resources Research*, 51, 5487-5503,  
17 10.1002/2015WR017062, 2015.
- 18 Bromwich, D. H.: Snowfall in high southern latitudes, *Reviews of Geophysics*, 26, 149-168,  
19 10.1029/RG026i001p00149, 1988.
- 20 Browning, S. A., and Goodwin, I. D.: Large-Scale Influences on the Evolution of Winter  
21 Subtropical Maritime Cyclones Affecting Australia's East Coast, *Monthly Weather Review*,  
22 141, 2416-2431, 10.1175/MWR-D-12-00312.1, 2013.
- 23 Browning, S. A., and Goodwin, I. D.: Large scale drivers of Australian East Coast Cyclones  
24 since 1871, *Australian Meteorological and Oceanographic Journal*, IN REVIEW - ESCCI  
25 Special Issue., 2015.
- 26 Callaghan, J., and Helman, P.: Severe storms on the east coast of Australia 1770-2008,  
27 Griffith Centre for Coastal Management, 2008.
- 28 Callaghan, J., and Power, S.: Variability and decline in the number of severe tropical  
29 cyclones making land-fall over eastern Australia since the late nineteenth century, *Climate*  
30 *Dynamics*, 37, 647-662, 10.1007/s00382-010-0883-2, 2011.



1 Callaghan, J., and Power, S.: Major coastal flooding in southeastern Australia 1860-2012,  
2 associated deaths and weather systems, *Australian Meteorological and Oceanographic*  
3 *Journal*, 64, 183-213, 2014.

4 Cook, E. R.: Using tree rings to study past El Nino/Southern Oscillation influences on  
5 climate, in: *El Nino : historical and paleoclimatic aspects of the southern oscillation* edited  
6 by: Diaz, H. F., and Markgraf, V., Accessed from <http://nla.gov.au/nla.cat-vn1812337>,  
7 Cambridge University Press, Cambridge [England] ; New York, NY, USA, 1992.

8 Cosgrove, W. J., and Loucks, D. P.: Water management: Current and future challenges and  
9 research directions, *Water Resources Research*, 51, 4823-4839, 10.1002/2014WR016869,  
10 2015.

11 Curran, M. A. J., van Ommen, T. D., and Morgan, V.: Seasonal characteristics of the major  
12 ions in the high-accumulation Dome Summit South ice core, Law Dome, Antarctica, in:  
13 *Annals of Glaciology*, Vol 27, 1998, edited by: Budd, W. F., *Annals of Glaciology*, Int  
14 *Glaciological Soc*, Cambridge, 385-390, 1998.

15 Delmotte, M., Masson, V., Jouzel, J., and Morgan, V. I.: A seasonal deuterium excess signal  
16 at Law Dome, coastal eastern Antarctica: A southern ocean signature, *Journal of Geophysical*  
17 *Research: Atmospheres*, 105, 7187-7197, 10.1029/1999JD901085, 2000.

18 Ding, Q., Steig, E. J., Battisti, D. S., and Wallace, J. M.: Influence of the Tropics on the  
19 Southern Annular Mode, *Journal of Climate*, 25, 6330-6348, 10.1175/JCLI-D-11-00523.1,  
20 2012.

21 Folland, C. K., Renwick, J. A., Salinger, M. J., and Mullan, A. B.: Relative influences of the  
22 Interdecadal Pacific Oscillation and ENSO on the South Pacific Convergence Zone,  
23 *Geophysical Research Letters*, 29, 10.1029/2001GL014201, 2002.

24 Gallant, A. J. E., and Gergis, J.: An experimental streamflow reconstruction for the River  
25 Murray, Australia, 1783–1988, *Water Resources Research*, 47, 10.1029/2010WR009832,  
26 2011.

27 Gallant, A. J. E., Kiem, A. S., Verdon-Kidd, D. C., Stone, R. C., and Karoly, D. J.:  
28 Understanding hydroclimate processes in the Murray-Darling Basin for natural resources  
29 management, *Hydrol. Earth Syst. Sci.*, 16, 2049-2068, 10.5194/hess-16-2049-2012, 2012.

30 Gergis, J., Gallant, A., Braganza, K., Karoly, D., Allen, K., Cullen, L., D'Arrigo, R.,  
31 Goodwin, I., Grierson, P., and McGregor, S.: On the long-term context of the 1997–2009  
32 'Big Dry' in South-Eastern Australia: insights from a 206-year multi-proxy rainfall  
33 reconstruction, *Climatic Change*, 111, 923-944, 10.1007/s10584-011-0263-x, 2012.

1 Goodwin, I. D., van Ommen, T. D., Curran, M. A. J., and Mayewski, P. A.: Mid latitude  
2 winter climate variability in the South Indian and southwest Pacific regions since 1300 AD,  
3 *Climate Dynamics*, 22, 783-794, 10.1007/s00382-004-0403-3, 2004.

4 Heinrich, I., Weidner, K., Helle, G., Vos, H., Lindesay, J., and Banks, J. C. G.: Interdecadal  
5 modulation of the relationship between ENSO, IPO and precipitation: insights from tree rings  
6 in Australia, *Climate Dynamics*, 33, 63-73, 10.1007/s00382-009-0544-5, 2009.

7 Hendon, H. H., Thompson, D. W. J., and Wheeler, M. C.: Australian Rainfall and Surface  
8 Temperature Variations Associated with the Southern Hemisphere Annular Mode, *Journal of*  
9 *Climate*, 20, 2452-2467, 10.1175/jcli4134.1, 2007.

10 Henley, B. J., Thyer, M. A., Kuczera, G., and Franks, S. W.: Climate-informed stochastic  
11 hydrological modeling: Incorporating decadal-scale variability using paleo data, *Water*  
12 *Resources Research*, 47, W11509, 10.1029/2010WR010034, 2011.

13 Ho, M., Kiem, A. S., and Verdon-Kidd, D. C.: The Southern Annular Mode: a comparison of  
14 indices, *Hydrol. Earth Syst. Sci.*, 16, 967-982, 10.5194/hess-16-967-2012, 2012.

15 Ho, M., Verdon-Kidd, D. C., Kiem, A. S., and Drysdale, R. N.: Broadening the Spatial  
16 Applicability of Paleoclimate Information—A Case Study for the Murray–Darling Basin,  
17 Australia, *Journal of Climate*, 27, 2477-2495, 10.1175/JCLI-D-13-00071.1, 2014.

18 Ho, M., Kiem, A. S., and Verdon-Kidd, D. C.: A paleoclimate rainfall reconstruction in the  
19 Murray-Darling Basin (MDB), Australia: 1. Evaluation of different paleoclimate archives,  
20 rainfall networks, and reconstruction techniques, *Water Resources Research*,  
21 10.1002/2015WR017058, 2015a.

22 Ho, M., Kiem, A. S., and Verdon-Kidd, D. C.: A paleoclimate rainfall reconstruction in the  
23 Murray-Darling Basin (MDB), Australia: 2. Assessing hydroclimatic risk using paleoclimate  
24 records of wet and dry epochs, *Water Resources Research*, 10.1002/2015WR017059, 2015b.

25 Ji, F., Evans, J., Argueso, D., Fita, L., and Di Luca, A.: Using large-scale diagnostic  
26 quantities to investigate change in East Coast Lows, *Climate Dynamics*, DOI  
27 10.1007/s00382-015-2481-9, 2015.

28 Jones, D. A., Wang, W., and Fawcett, R.: High-quality spatial climate data-sets for Australia,  
29 *Australian Meteorological and Oceanographic Journal*, 58, 233-248, 2009.

30 Karoly, D. J.: Southern Hemisphere Circulation Features Associated with El Niño-Southern  
31 Oscillation Events, *Journal of Climate*, 2, 1239-1252, 10.1175/1520-  
32 0442(1989)002<1239:shcfaw>2.0.co;2, 1989.

33 Kiem, A. S., and Franks, S. W.: On the identification of ENSO-induced rainfall and runoff  
34 variability: a comparison of methods and indices, *Hydrological Sciences*, 46, 1-13, 2001.

1 Kiem, A. S., Franks, S. W., and Kuczera, G.: Multi-decadal variability of flood risk,  
2 Geophysical Research Letters, 30, 1035, 10.1029/2002GL015992, 2003.

3 Kiem, A. S., and Franks, S. W.: Multi-decadal variability of drought risk, eastern Australia,  
4 Hydrological Processes, 18, 2039-2050, 10.1002/hyp.1460, 2004.

5 Kiem, A. S., and Verdon-Kidd, D. C.: Steps toward “useful” hydroclimatic scenarios for  
6 water resource management in the Murray-Darling Basin, Water Resources Research, 47,  
7 10.1029/2010WR009803, 2011.

8 Kiem, A. S., and Verdon-Kidd, D. C.: The importance of understanding drivers of  
9 hydroclimatic variability for robust flood risk planning in the coastal zone, Australian Journal  
10 of Water Resources, 17, 126-134, 2013.

11 Kiem, A. S., Twomey, C., Lockart, N., Willgoose, G., Kuczera, G., Chowdhury, A. F. M. K.,  
12 Parana Manage, N., and Zhang, L.: Links between East Coast Lows (ECLs) and the spatial  
13 and temporal variability of rainfall along the eastern seaboard of Australia (ESA), Australian  
14 Meteorological and Oceanographic Journal, IN REVIEW - ESCCI Special Issue., 2015.

15 L’Heureux, M. L., and Thompson, D. W. J.: Observed Relationships between the El Niño–  
16 Southern Oscillation and the Extratropical Zonal-Mean Circulation, Journal of Climate, 19,  
17 276-287, 10.1175/JCLI3617.1, 2006.

18 Lavery, B., Joung, G., and Nicholls, N.: An extended high-quality historical rainfall dataset  
19 for Australia, Australian Meteorological Magazine, 46, 27-38, 1997.

20 Lough, J. M.: Great Barrier Reef coral luminescence reveals rainfall variability over  
21 northeastern Australia since the 17th century, Paleoceanography, 26,  
22 10.1029/2010PA002050, 2011.

23 Masson-Delmotte, V., Delmotte, M., Morgan, V., Etheridge, D., van Ommen, T., Tartarin, S.,  
24 and Hoffmann, G.: Recent southern Indian Ocean climate variability inferred from a Law  
25 Dome ice core: new insights for the interpretation of coastal Antarctic isotopic records,  
26 Climate Dynamics, 21, 153-166, 10.1007/s00382-003-0321-9, 2003.

27 McDonald, J.: Climate Controls on Trace Element Variability in Cave Drip Waters and  
28 Calcite: A Modern Study from Two Karst Systems in S.E. Australia, School of Environment  
29 and Life Sciences, University of Newcastle, Newcastle, Australia, 2005.

30 McDonald, J., Drysdale, R., Hodge, E., Hua, Q., Fischer, M. J., Treble, P. C., Greig, A., and  
31 Hellstrom, J. C.: One thousand year palaeohydrological record derived from SE Australian  
32 stalagmites, EGU General Assembly 2009, Vienna, 2009, 11554 pp.,

33 McDonald, J., Drysdale, R., Hua, Q., Hodge, E., Treble, P. C., Greig, A., Fallon, S., Lee, S.,  
34 and Hellstrom, J. C.: A 1500 year southeast Australian rainfall record based on speleothem

1 hydrological proxies, AMOS Annual Conference 2013 - Sense and Sensitivity, Melbourne,  
2 Australia, 11-13 February, 2013, 2013.

3 McGowan, H. A., Marx, S. K., Denholm, J., Soderholm, J., and Kamber, B. S.:  
4 Reconstructing annual inflows to the headwater catchments of the Murray River, Australia,  
5 using the Pacific Decadal Oscillation, *Geophysical Research Letters*, 36,  
6 10.1029/2008GL037049, 2009.

7 Mo, K. C., and Higgins, R. W.: The Pacific–South American Modes and Tropical Convection  
8 during the Southern Hemisphere Winter, *Monthly Weather Review*, 126, 1581-1596,  
9 10.1175/1520-0493(1998)126<1581:TPSAMA>2.0.CO;2, 1998.

10 Mortazavi-Naeini, M., Kuczera, G., Kiem, A. S., Cui, L., Henley, B., Berghout, B., and  
11 Turner, E.: Robust optimization to secure urban bulk water supply against extreme drought  
12 and uncertain climate change, *Environmental Modelling & Software*, 69, 437-451,  
13 <http://dx.doi.org/10.1016/j.envsoft.2015.02.021>, 2015.

14 Mudelsee, M.: Estimating Pearson's Correlation Coefficient with Bootstrap Confidence  
15 Interval from Serially Dependent Time Series, *Mathematical Geology*, 35, 651-665,  
16 10.1023/B:MATG.0000002982.52104.02, 2003.

17 Neukom, R., and Gergis, J.: Southern Hemisphere high-resolution palaeoclimate records of  
18 the last 2000 years, *The Holocene*, 22, 501-524, 10.1177/0959683611427335, 2012.

19 Palmer, A. S., van Ommen, T. D., Curran, M. A. J., Morgan, V., Souney, J. M., and  
20 Mayewski, P. A.: High-precision dating of volcanic events (A.D. 1301–1995) using ice cores  
21 from Law Dome, Antarctica, *Journal of Geophysical Research: Atmospheres*, 106, 28089-  
22 28095, 10.1029/2001JD000330, 2001.

23 Pepler, A., Coutts-Smith, A., and Timbal, B.: The role of East Coast Lows on rainfall patterns  
24 and inter-annual variability across the East Coast of Australia, *International Journal of*  
25 *Climatology*, 34, 1011-1021, 10.1002/joc.3741, 2014a.

26 Pepler, A. S., Di Luca, A., Ji, F., Alexander, L. V., Evans, J. P., and Sherwood, S. C.: Impact  
27 of Identification Method on the Inferred Characteristics and Variability of Australian East  
28 Coast Lows, *Monthly Weather Review*, 143, 864-877, 10.1175/MWR-D-14-00188.1, 2014b.

29 Plummer, C. T., Curran, M. A. J., van Ommen, T. D., Rasmussen, S. O., Moy, A. D., Vance,  
30 T. R., Clausen, H. B., Vinther, B. M., and Mayewski, P. A.: An independently dated 2000-yr  
31 volcanic record from Law Dome, East Antarctica, including a new perspective on the dating  
32 of the 1450s CE eruption of Kuwae, Vanuatu, *Clim. Past*, 8, 1929-1940, 10.5194/cp-8-1929-  
33 2012, 2012.

1 Power, S., Casey, T., Folland, C., Colman, A., and Mehta, V.: Inter-decadal modulation of  
2 the impact of ENSO on Australia, *Climate Dynamics*, 15, 319-324, 10.1007/s003820050284,  
3 1999a.

4 Power, S., Tseitkin, F., Mehta, V., Lavery, B., Torok, S., and Holbrook, N.: Decadal climate  
5 variability in Australia during the twentieth century, *International Journal of Climatology*, 19,  
6 169-184, 10.1002/(sici)1097-0088(199902)19:2<169::aid-joc356>3.0.co;2-y, 1999b.

7 Razavi, S., Elshorbagy, A., Wheater, H., and Sauchyn, D.: Toward understanding  
8 nonstationarity in climate and hydrology through tree ring proxy records, *Water Resources*  
9 *Research*, 1813-1830, 10.1002/2014WR015696, 2015.

10 Risbey, J. S., Pook, M. J., McIntosh, P. C., Wheeler, M. C., and Hendon, H. H.: On the  
11 Remote Drivers of Rainfall Variability in Australia, *Monthly Weather Review*, 137, 3233-  
12 3253, 2009.

13 Roberts, J., Plummer, C., Vance, T. R., van Ommen, T., Moy, A., Poynter, S., Treverrow, A.,  
14 Curran, M., and George, S.: A 2000-year annual record of snow accumulation rates for Law  
15 Dome, East Antarctica, *Clim. Past*, 11, 697-707, 10.5194/cp-11-697-2015, 2015.

16 Speer, M. S.: On the late twentieth century decrease in Australian east coast rainfall extremes,  
17 *Atmospheric Science Letters*, 9, 160-170, 2008.

18 Speer, M. S., Wiles, P., and Pepler, A.: Low pressure systems off the New South Wales coast  
19 and associated hazardous weather: establishment of a database, *Australian Meteorological*  
20 *and Oceanographic Journal*, 58, 29-39, 2009.

21 Timbal, B.: The climate of the Eastern Seaboard of Australia: A challenging entity now and  
22 for future projections, *IOP Conference Series: Earth and Environmental Science*, 11, 012013,  
23 2010.

24 Tozer, C. R., Kiem, A. S., and Verdon-Kidd, D. C.: On the uncertainties associated with  
25 using gridded rainfall data as a proxy for observed, *Hydrol. Earth Syst. Sci.*, 16, 1481-1499,  
26 10.5194/hess-16-1481-2012, 2012.

27 Twomey, C., and Kiem, A. S.: Spatial and temporal inhomogeneity of rainfall patterns in  
28 Australia - why is the eastern seaboard of Australian (ESA) different and why does  
29 inhomogeneity also exist within the ESA?, *International Journal of Climatology*, IN  
30 REVIEW., 2015a.

31 Twomey, C., and Kiem, A. S.: East Coast Lows (ECLs) and rainfall along the eastern  
32 seaboard of Australia (ESA) - comparison of datasets used to record ECL occurrence and  
33 impacts on rainfall, *Monthly Weather Review*, IN PREPARATION., 2015b.

1 van Ommen, T. D., and Morgan, V.: Calibrating the ice core paleothermometer using  
2 seasonality, *Journal of Geophysical Research: Atmospheres*, 102, 9351-9357,  
3 10.1029/96JD04014, 1997.

4 van Ommen, T. D., and Morgan, V.: Snowfall increase in coastal East Antarctica linked with  
5 southwest Western Australian drought, *Nature Geosci*, 3, 267-272, 10.1038/ngeo761, 2010.

6 Vance, T. R., van Ommen, T. D., Curran, M. A. J., Plummer, C. T., and Moy, A. D.: A  
7 Millennial Proxy Record of ENSO and Eastern Australian Rainfall from the Law Dome Ice  
8 Core, East Antarctica, *Journal of Climate*, 26, 710-725, 10.1175/JCLI-D-12-00003.1, 2013.

9 Vance, T. R., Roberts, J. L., Plummer, C. T., Kiem, A. S., and van Ommen, T. D.:  
10 Interdecadal Pacific variability and eastern Australian megadroughts over the last  
11 millennium, *Geophysical Research Letters*, 42, 129-137, 10.1002/2014GL062447, 2015.

12 Vance, T. R., Roberts, J. L., Moy, A. D., Curran, M. A. J., Tozer, C. R., Gallant, A. J. E.,  
13 Abram, N. J., van Ommen, T. D., Young, D. A., Grima, C., Blankenship, D. D., and Siegert,  
14 M. J.: Optimal site selection for a high-resolution ice core record in East Antarctica, *Clim.*  
15 *Past*, 12, 595-610, 10.5194/cp-12-595-2016, 2016.

16 Verdon-Kidd, D. C., and Kiem, A. S.: Nature and causes of protracted droughts in southeast  
17 Australia: Comparison between the Federation, WWII, and Big Dry droughts, *Geophysical*  
18 *Research Letters*, 36, L22707, 10.1029/2009gl041067, 2009.

19 Verdon-Kidd, D. C., and Kiem, A. S.: Quantifying Drought Risk in a Nonstationary Climate,  
20 *Journal of Hydrometeorology*, 11, 1019-1031, 10.1175/2010jhm1215.1, 2010.

21 Verdon, D. C., Wyatt, A. M., Kiem, A. S., and Franks, S. W.: Multidecadal variability of  
22 rainfall and streamflow: Eastern Australia, *Water Resources Research*, 40,  
23 10.1029/2004wr003234, 2004.

24 Verdon, D. C., and Franks, S. W.: Indian Ocean sea surface temperature variability and  
25 winter rainfall: Eastern Australia, *Water Resources Research*, 41, 10.1029/2004wr003845,  
26 2005.

27 Verdon, D. C., and Franks, S. W.: Long-term behaviour of ENSO: Interactions with the PDO  
28 over the past 400 years inferred from paleoclimate records, *Geophysical Research Letters*, 33,  
29 L06712, 10.1029/2005GL025052, 2006.

30 Verdon, D. C., and Franks, S. W.: Long-term drought risk assessment in the Lachlan River  
31 Valley - a paleoclimate perspective, *Australian Journal of Water Resources*, 11, 145-152,  
32 2007.

1 Whan, K., Timbal, B., and Lindesay, J.: Linear and nonlinear statistical analysis of the impact  
2 of sub-tropical ridge intensity and position on south-east Australian rainfall, *International*  
3 *Journal of Climatology*, 10.1002/joc.3689, 2013.

4

5

1 Table 1. Pearson correlation values between LD<sub>SSS</sub> and 12 month average (October-September)  
 2 rainfall recorded at gauge 61010 and the AWAP WR catchment average for the 1900-2010  
 3 period and IPO phases. Bootstrap 95% confidence intervals are also indicated (Mudelsee,  
 4 2003). Bold values are significant at 95%.

Time Period	61010	AWAP catchment average
Full record (1900-2010)	<b>0.29</b> [0.12 – 0.45]	<b>0.28</b> [0.10 – 0.44]
IPO positive (1924-1941, 1979-1997)	<b>0.47</b> [0.23 – 0.66]	<b>0.55</b> [0.31 – 0.73]
IPO positive (1924-1941)	<b>0.33</b> [0.01 – 0.59]	0.34 [-0.11 – 0.68]
IPO positive (1979-1997)	<b>0.59</b> [0.23 – 0.81]	<b>0.67</b> [0.44 – 0.82]
IPO negative (1947-1975)	<b>0.37</b> [0.13 – 0.57]	<b>0.32</b> [0.06 – 0.54]

5

6



1 Table 2. Root Mean Square Error in mm/year (%) and Reduction in Error between the rainfall  
 2 reconstruction and 12 month average (October-September) rainfall recorded at gauge 61010  
 3 and the AWAP WR catchment average for the 1900-2010 period and IPO phases.

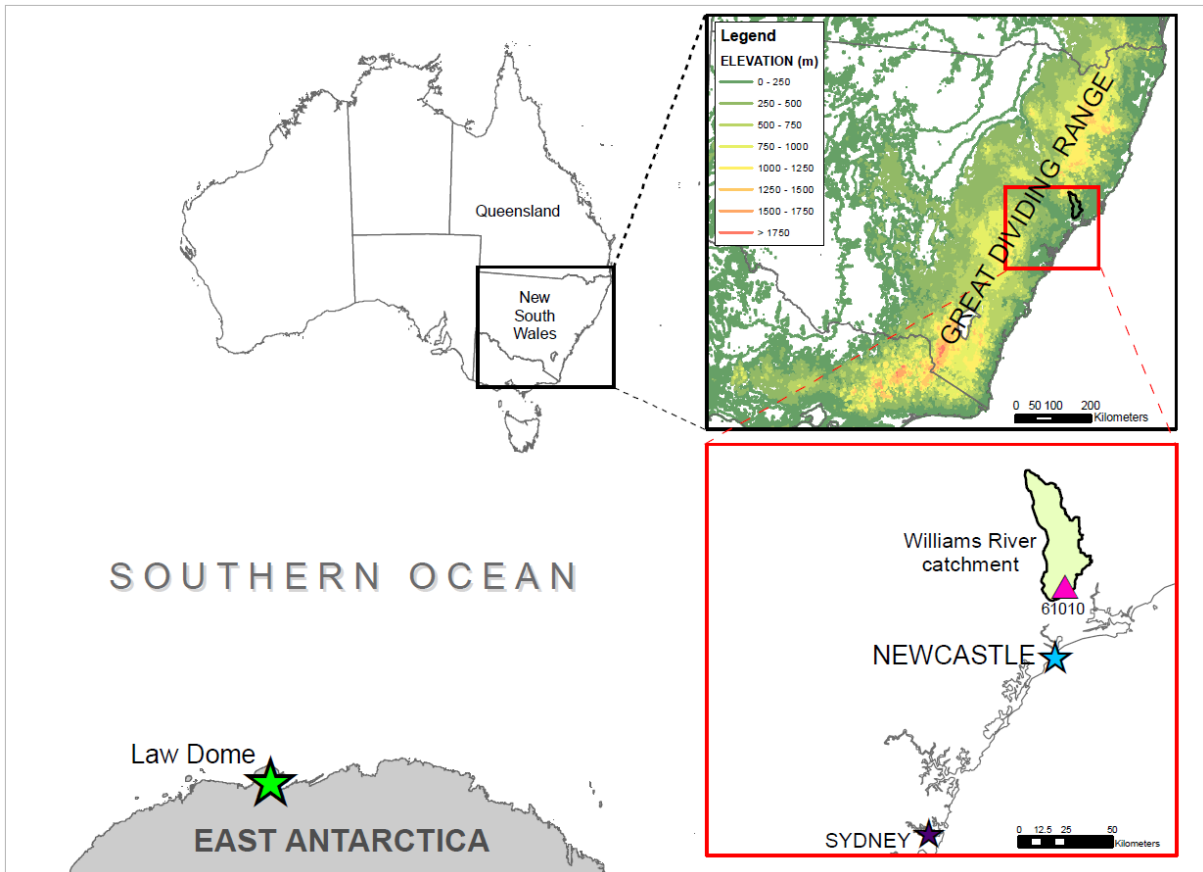
Time Period	61010		AWAP catchment average	
	RMSE mm (%)	RE	RMSE mm (%)	RE
Full record (1900-2010)	267 (25.1)	0.07	254 (23.1)	0.08
IPO positive (1924-1941, 1979-1997)	239 (22.5)	0.14	202 (18.4)	0.25
IPO positive (1924-1941)	254 (23.9)	0.10	187 (17.0)	0.08
IPO positive (1979-1997)	223 (21.0)	0.11	216 (19.6)	0.33
IPO negative (1947-1975)	254 (23.9)	0.10	306 (27.8)	0.02

4

5

1 Table 3. Duration of longest dry and wet periods for the AWAP and reconstructed rainfall.

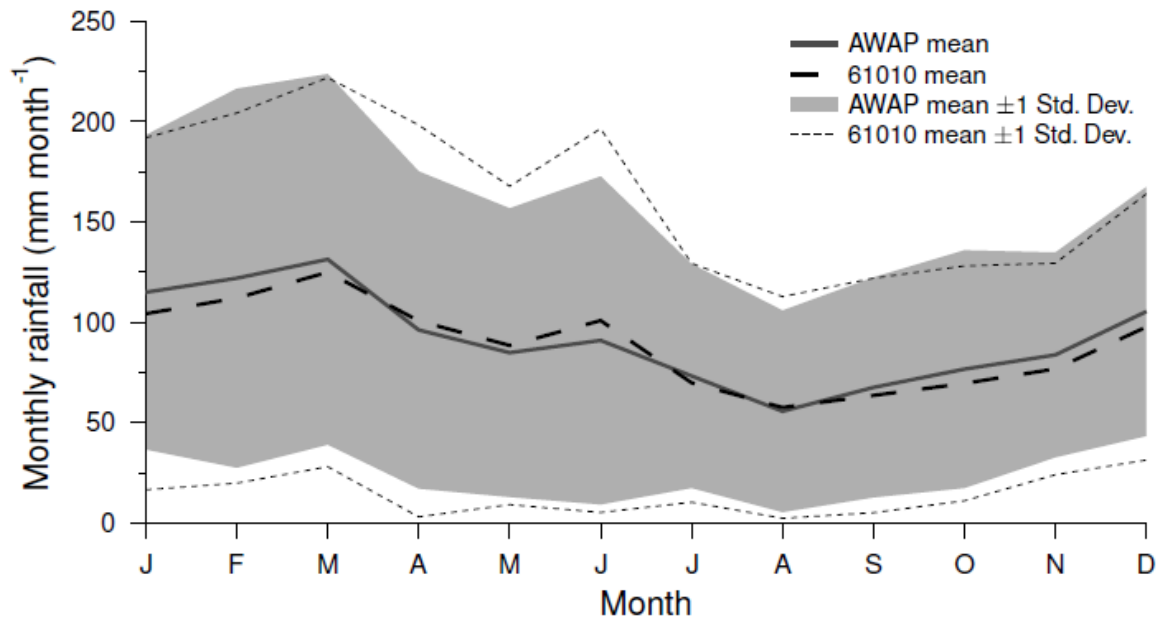
Mean (mm) used to determine wet/dry	Std. Dev. (mm) used to determine wet/dry	$x$ value used to determine wet/dry (Threshold = Mean $\pm$ $x$ *Std. Dev.)	Duration of longest DRY period (years)	DRY period	Duration of longest WET period (years)	WET period <sup>2</sup> 3
<b>A</b> AWAP catchment average rainfall (1900-2010)						
1100.0	264.6	0 (Mean)	8	1935-1942	5	1927-1931
(1900-2010)	(1900-2010)	0.1	8	1935-1942	8	1925-1932
		0.2	8	1935-1942	8	1925-1932
		0.3	8	1935-1942	8	1925-1932
		0.4	8	1935-1942	9	1948-1956
		0.5	9	1979-1987	9	1924-1932, 1948-1956, 1971-1979
<b>B</b> Reconstructed Rainfall (1900-2010)						
1100.0	73.9	0 (Mean)	7	1936-1942	7	1907-1913
(1900-2010)	(1900-2010)	0.1	7	1936-1942	8	1907-1914
		0.2	8	1935-1942	10	1905-1914
		0.3	8	1935-1942	10	1905-1914
		0.4	9	1973-1981	10	1905-1914
		0.5	11	1973-1983	10	1905-1914
<b>C</b> Reconstructed Rainfall (1000-2012)						
1100.0	73.9	0 (Mean)	7	1936-1942	16	1499-1605, 1834-1849
(1900-2010)	(1900-2010)	0.1	9	1215-1223	26	1831-1856
		0.2	9	1215-1223	27	1830-1856
		0.3	12	1193-1204	39	1830-1868
		0.4	12	1193-1204	39	1830-1868
		0.5	12	1193-1204, 1212-1223	39	1830-1868
<b>D</b> Reconstructed Rainfall (1000-2012)						
1126.1	83.0	0 (Mean)	12	1193-1204	16	1834-1849
(1000-2012)	(1000-2012)	0.1	12	1193-1204	16	1834-1849
		0.2	12	1193-1204	16	1834-1849
		0.3	17	1117-1133	16	1589-1605, 1834-1849
		0.4	17	1117-1133	26	1831-1856
		0.5	18	1206-1223	27	1830-1856



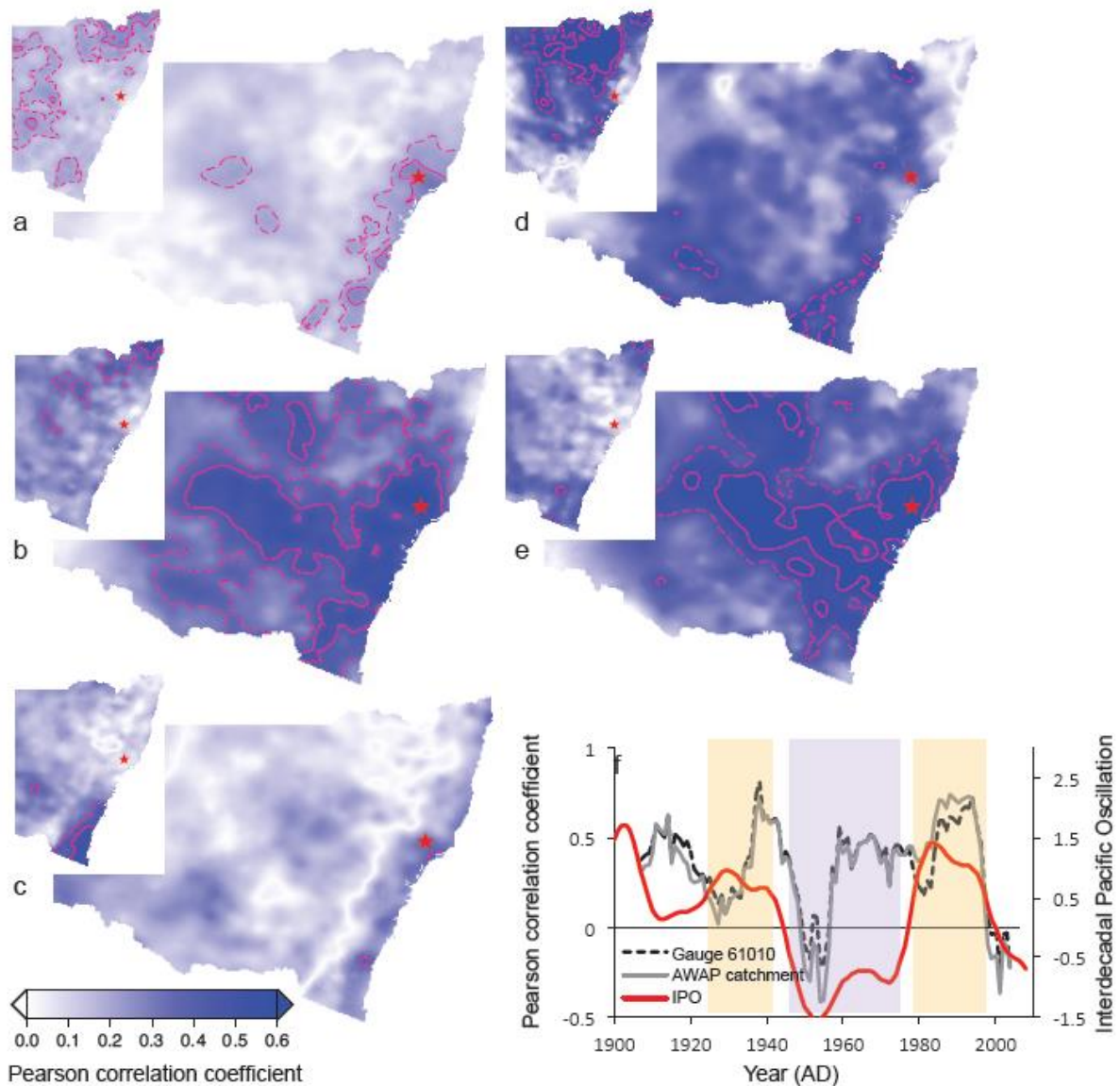
1

2 Figure 1. Location of Law Dome in relation to Australia with insets indicating the Great  
 3 Dividing Range, WR catchment boundary and the location of 61010 high quality rainfall gauge,  
 4 Newcastle and Sydney.

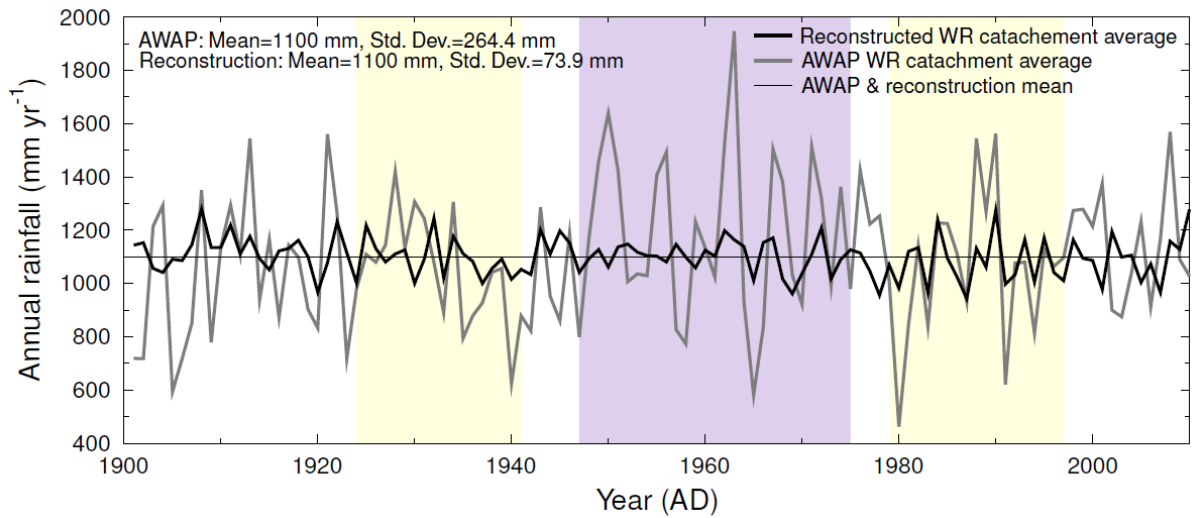
5



1  
 2 Figure 2. Climatology of WR catchment rainfall. Shown is the mean and standard deviation of  
 3 monthly rainfall recorded at the 61010 gauge and for the AWAP catchment average.  
 4

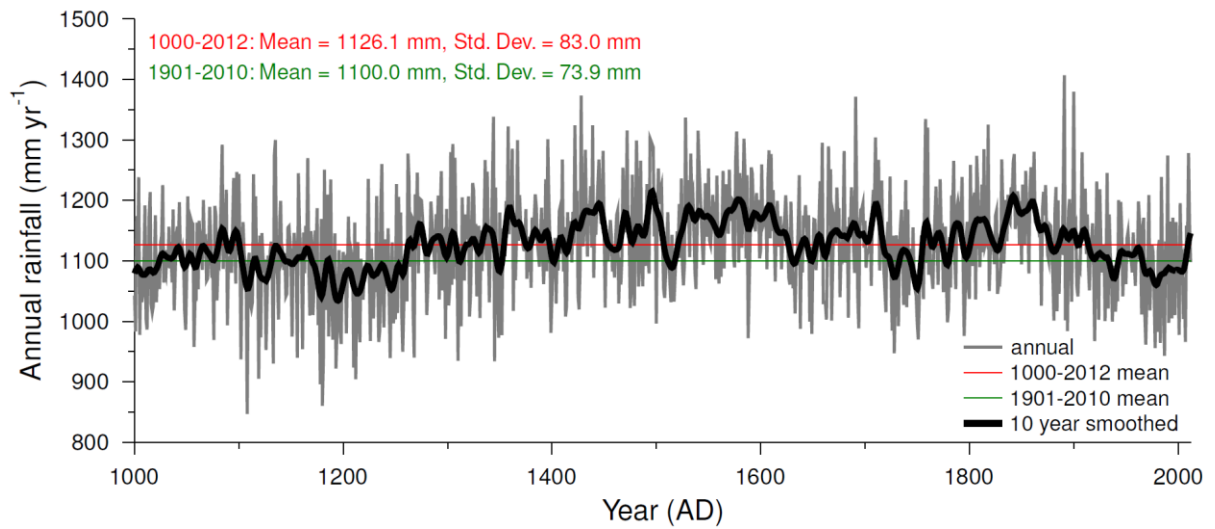


1  
 2 Figure 3. Correlations between (a) 12 month average (October-September) AWAP rainfall and  
 3 LD<sub>SS</sub> for the 1900-2010 period with inset showing correlations between annual AWAP rainfall  
 4 calculated from January-December and LD<sub>SS</sub> for 1900-2010 period, (b) as in (a) but for the  
 5 combined IPO positive phases (1924-1941, 1979-1997), (c) as in (a) but for the IPO negative  
 6 phase (1947-1975), (d) as in (a) but for the first IPO positive (1924-1941) phase (e) as in (a)  
 7 but for the second IPO positive (1979-1997) phase and (f) 13 year moving window correlations  
 8 between 12 month average (October-September) rainfall recorded at gauge 61010 and the  
 9 AWAP WR catchment average and LD<sub>SS</sub> with shading indicating IPO positive (yellow) and  
 10 IPO negative (purple) phases (red line shown indicates 13 year smoothed instrumental IPO  
 11 record). Note that for (a) – (e) the star represents the location of the WR catchment centroid,  
 12 dashed pink line shows 95% significance level, bold pink line shows 99% significance level.

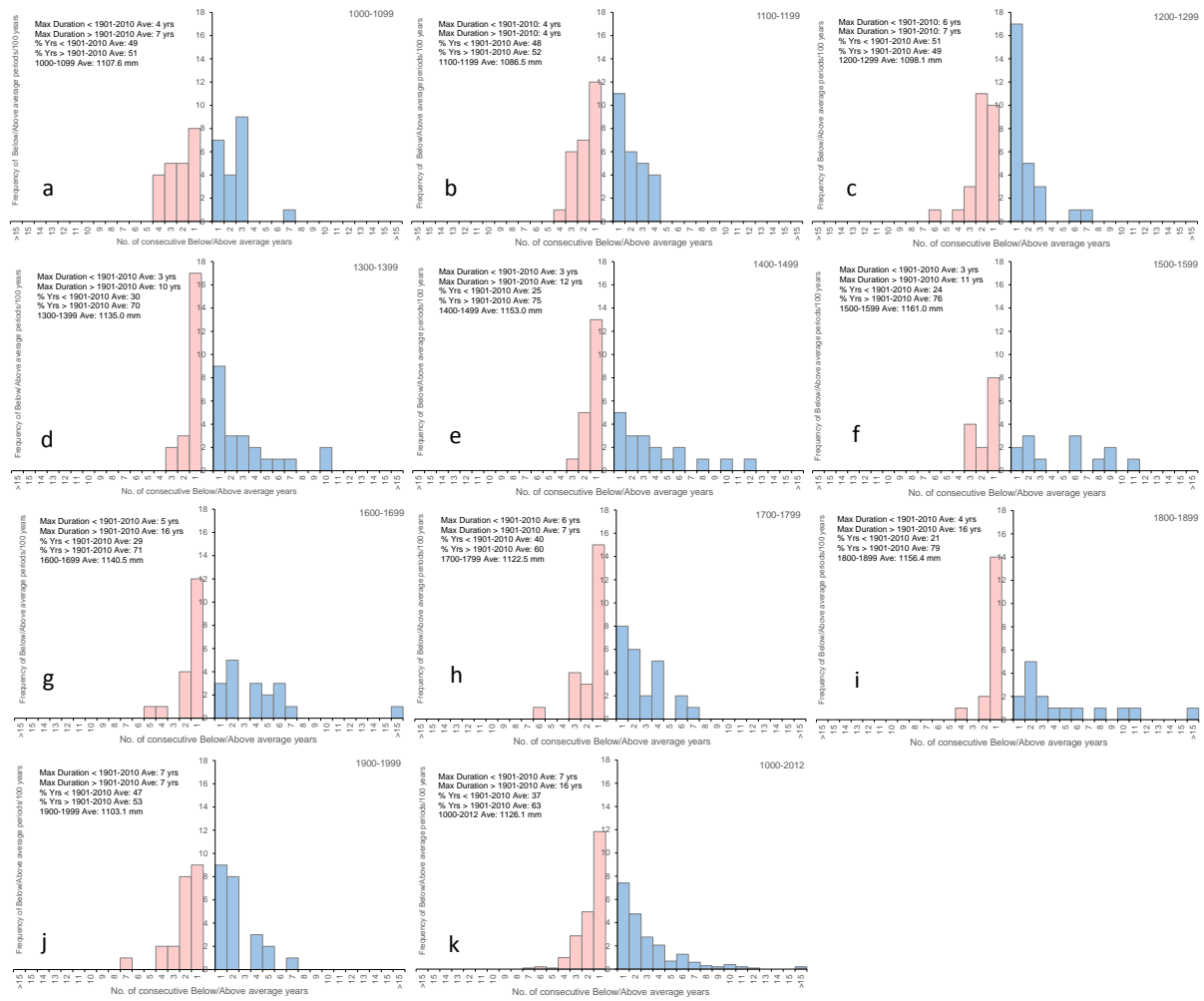


1  
 2 Figure 4. Reconstructed (thick black), AWAP (grey) WR catchment average rainfall and  
 3 reconstruction/AWAP mean (thin black). Shading indicates IPO positive (yellow) and IPO  
 4 negative (purple) phases.

5



1  
 2 Figure 5. WR catchment rainfall reconstruction (grey line), 10 year Gaussian smooth (bold  
 3 black line), mean of the rainfall reconstruction for 1000-2012 period (red line) and 1900-2010  
 4 period (green line).  
 5



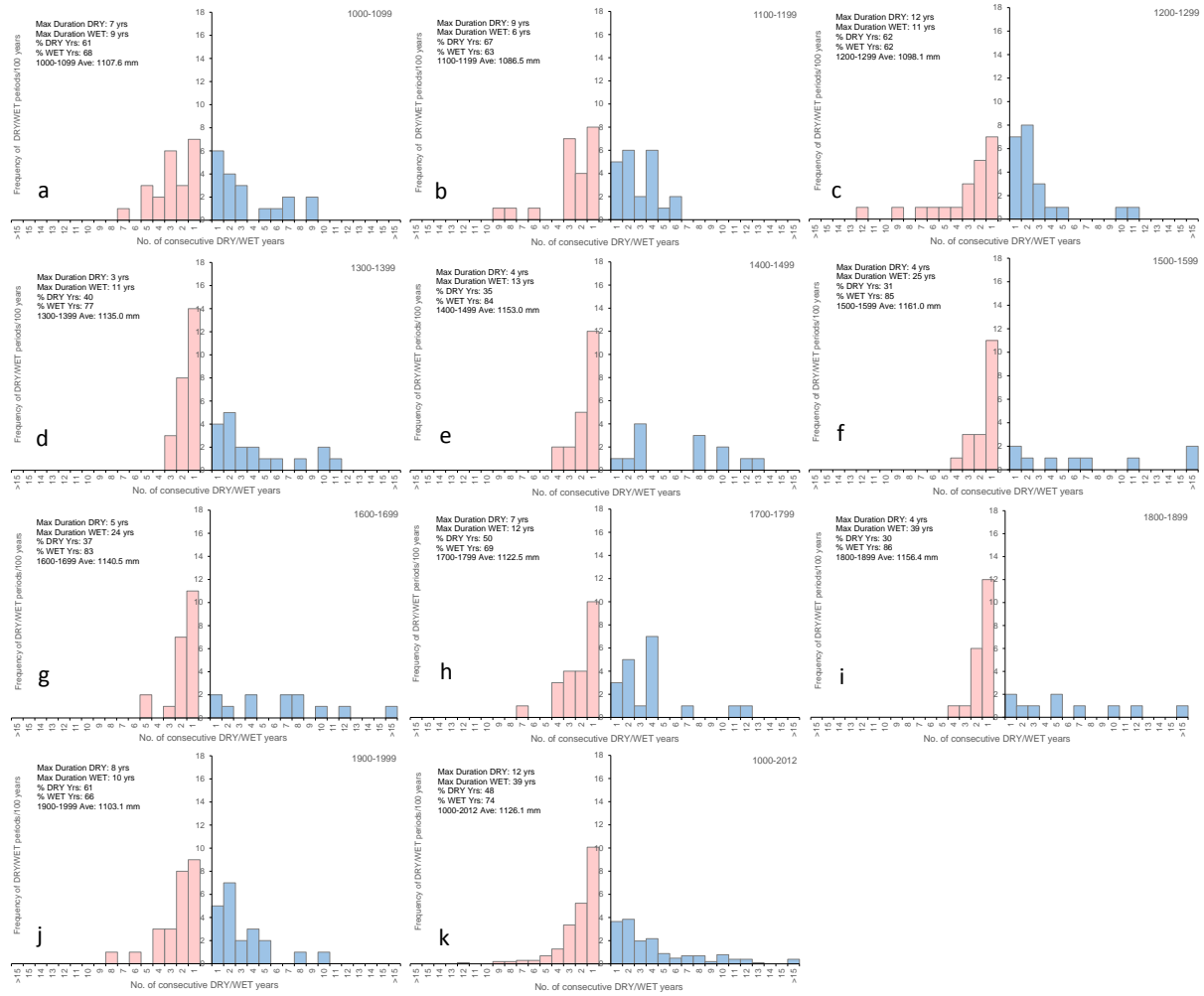
1

2

Figure 6. Histograms of duration of above (blue) and below (pink) average rainfall periods in each century since CE 1000. a-j are centennial subsets and k is the CE 1000-2012 period (note different axis scaling). Above/below average are defined using  $x = 0$  in Eq. 1 (as per Table 2).

5





1  
2  
3  
4  
5  
6  
7

Figure 7. Histograms of duration of WET (blue) and DRY (pink) average periods during each century since CE 1000. a-j are centennial subsets and k is the CE 1000-2012 period (note different axis scaling). WET/DRY are defined using  $x = 0.3$  in Eq. 1 (as per Table 2).